2-Alkoxycarbonylpyridinium N-Aminides: 1,3-Dipoles or 1,4-Nucleophile−Electrophile Synthons? Experimental and Theoretical Evidence for the Mechanism of Pyrido[1,2-*b*]pyridazinium Inner Salt Formation†

Jesús Valenciano,‡ Ana M. Cuadro,‡ Juan J. Vaquero,‡ Julio Alvarez-Builla,*,‡ Raul Palmeiro,§ and Obis Castaño§

Departamento de Química Orgánica and Departamento de Química Física, Universidad de Alcalá, 28871-Alcalá de Henares, Madrid, Spain

Received June 16, 1999

2-Alkoxycarbonylpyridinium *N*-aminides behave as 1,3-dipoles toward acetylenic compounds and as 1,4-nucleophile−electrophiles with heterocumulenes in a [4 + 2] cyclocondensation process, yielding in the latter case conjugated mesomeric betaines. These *N*-aminides also behave as 1,3-dipoles when reacted with olefinic dipolarophiles, producing the corresponding cycloadducts that, depending on their regioisomeric nature, subsequently undergo a ring expansion process to produce pyrido[1,2-*b*]pyridazinium inner salts. A mechanistic investigation performed using both PM3 frontier molecular orbital (FMO) and potential energy surface (PES) analysis at the RHF/6-31+G* level indicates that both the cycloaddition reaction and the ring expansion occur in a concerted way rather than through a stepwise mechanism via a zwitterionic intermediate.

The heterocyclic mesomeric betaines[1] **1** are established, versatile 1,3-dipoles that are involved in 1,3-dipolar cycloaddition reactions.[2] 2-Alkyl- and 2-amino-substituted structures **2** have the potential to function as 1,4-dinucleophiles via deprotonation and are capable of reacting with 1,2-dicarbonyl compounds (Westphal reaction)[3] to afford a variety of azonia derivatives possessing a quaternary bridgehead nitrogen.[4] In contrast, relatively less attention has been focused on the possibility of using compounds **3** as 1,4-nucleophile−electrophiles[5] (Chart 1) to produce new conjugated mesomeric betaines.

Chart 1

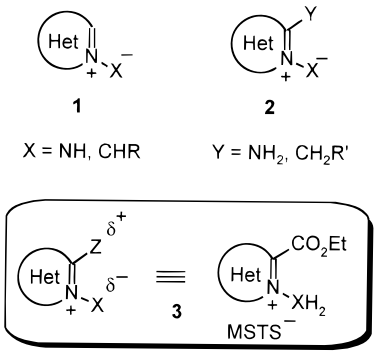

MSTS = Mesitylenesulfonate

We previously reported[6] one of the few examples of the 1,4-nucleophile−electrophile character of **3**, exemplified by the 2-ethoxycarbonyl azinium salts **3**, which on reaction with isocyanates and isothiocyanates afforded new conjugated mesomeric betaines **6** in a [4 + 2] cyclocondensation process. It has also been reported, however, that the *N*-aminides **4** behave as 1,3-dipoles when reacted with ethyl propiolate to afford the corresponding cycloadduct[7] **7** (Scheme 1). This apparent dual role prompted us to explore the reactivity of **3** with different olefinic dipolarophiles to gain further insight into its behavior.

We found that *N*-aminides **4** behave as 1,3-dipoles when reacted with typical Michael acceptors, giving rise to the corresponding cycloadducts that, depending on their regioisomeric nature, subsequently undergo a ring expansion process,[8] leading to the formation of conjugated mesomeric betaines, the isolated products from these reactions.

† Dedicated to Professor José Elguero on the occasion of his 65th birthday.

* Corresponding author. FAX: 34-1-91-8854660. E-mail: jalvarez@quimor.alcala.es.

‡ Departamento de Química Orgánica.

§ Departamento de Química Física.

(1) Ollis, W. D.; Stanforth, S. P. *Tetrahedron* **1985**, *41*, 2239.

(2) Padwa, A. in *1,3-Dipolar Cycloaddition Chemistry*; Taylor, E. C., Weissberger, A., Eds.; J. Wiley & Sons: New York, 1984.

(3) Westphal, O.; Jahn, K.; Heffe, W. E. *Arch. Pharm.* **1961**, *294*, 37.

(4) For recent contributions, see: (a) Matia, M. P.; Ezquerra, J.; Sanchez-Ferrando, F.; Garcia-Navio, J. L.; Vaquero, J. J.; Alvarez-Builla, J.*Tetrahedron* **1991**, *47*, 7329. (b) Matia, M. P.; Ezquerra, J.; Sanchez-Ferrando, F.; Garcia-Navio J. L.; Vaquero, J. J.; Alvarez-Builla, J. *Tetrahedron Lett.* **1991**, *32*, 7575. (c) Hajós, G.; Messmer, A.; Bátori, S.; Riedl, Z. *Bull.* Soc. Chem. **1992**, *101*, 597. (d) Hajós, G.; Riedl, Z.; Gács-Baitz, E.; Messmer, A. *Tetrahedron* **1992**, *48*, 8459. (e) Matia, M. P.; Garcia-Navio, J. L.; Vaquero, J. J.; Alvarez-Builla, J. *Liebigs Ann. Chem*. **1992**, 777. (f) Santiesteban, I.; Siro, J. G.; Vaquero, J. J.; Garcia-Navio, J. L.; Alvarez-Builla, J.; Castaño. O. *J. Org. Chem*. **1995**, *60*, 5667. (g) Diaz, A.; Matia, M. P.; Garcia, J. L.; Vaquero, J. J.; Alvarez-Builla, J. *J. Org. Chem*. **1995**, *59*, 8294. (h) Molina, A.; Vaquero, J. J.; Garcia-Navio, J. L.; Alvarez-Builla, J.; Rodrigo, M. M.; Castaño, O.; de Andrés, J. L. *Bioorg., Med. Chem. Lett*. **1996**, 1453. (i) Pastor, J.; Siro, J.; García-Navio, J. L.; Alvarez-Builla, J.; Gago, F.; de Pascual-Teresa, B.; Pastor, M.; Rodrigo, M. *J. Org. Chem*. **1997**, *62*, 5476. (j) Molina, A.; Vaquero J. J.; Garcia-Navio, J. L.; Alvarez-Builla, J.; de Pascual-Teresa, B.; Gago, F.; Rodrigo, M. M. *J. Org. Chem*. **1999** (in press).

(5) (a) Bátori, S.; Juhász-Riedl, Zs.; Sandor, P.; Messmer, A. *J. Heterocycl. Chem*. **1986**, *23*, 375. (b) Bátori, S.; Messmer, A. *J. Heterocycl. Chem*. **1988**, *25*, 437. (c) Bátori, S.; Hajós, G.; Sándor, P.; Messmer, A. *J. Org. Chem*. **1989**, *54*, 3062. (d) Bátori, S.; Messmer, A. *J. Heterocycl. Chem*. **1990**, *27*, 1673.

(6) Cuadro, A. M.; Valenciano, J.; Vaquero, J. J.; Garcia, J. L.; Alvarez-Builla, J. *Tetrahedron* **1993**, *49*, 3185.

(7) Boekelheide, V.; Feddoruk, N. *J. Org. Chem*. **1968**, *33*, 2062.

(8) Valenciano, J.; Cuadro, A. M.; Vaquero, J. J.; Alvarez-Builla, J. *Tetrahedron Lett*. **1999**, 763.

10.1021/jo9909655 CCC: $18.00
Published on Web 11/16/1999

Scheme 1

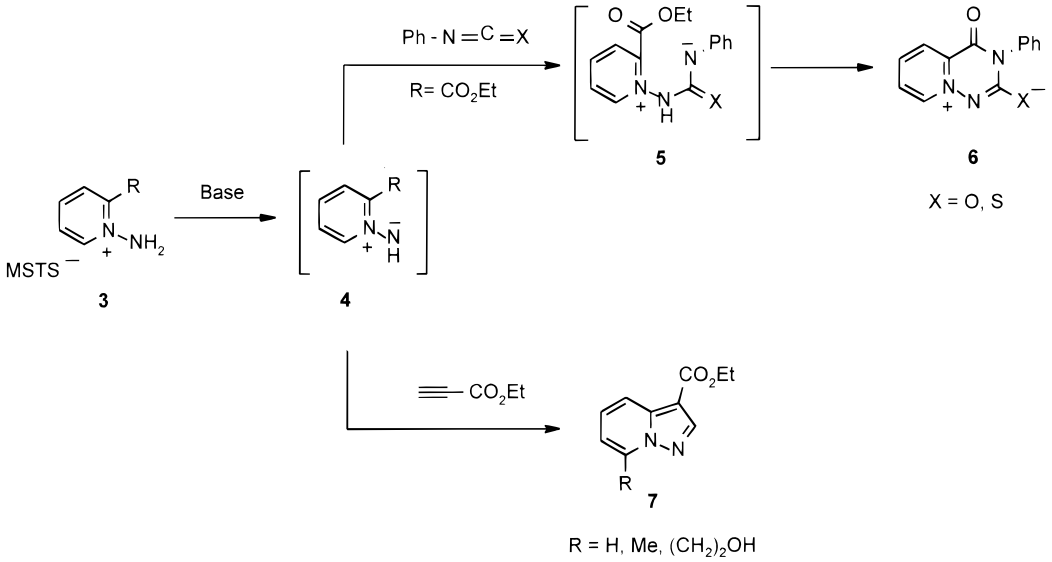

Scheme 2

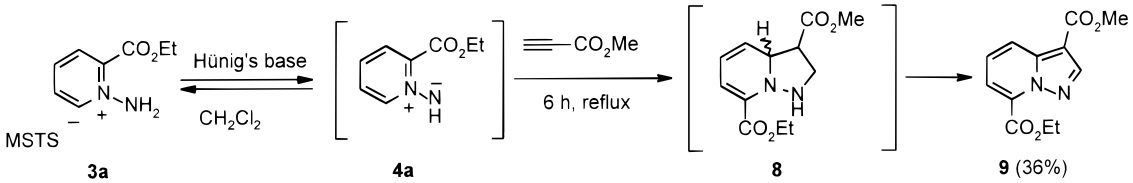

As several key questions emerged from these experimental observations, a theoretical study based on PM3 frontier molecular orbital (FMO) and potential energy surface (PES) analysis at the RHF/6-31+G* level was performed to examine the cycloadduct formation and to find a reaction path that accounts for the experimental behavior of *N*-aminides **4**.

Computational Methods

The semiempirical computations were performed with MOPAC93[9] using a PM3[10] Hamiltonian function. The purpose of the semiempirical computations was to achieve approximated geometries of some stationary points and to obtain the atomic orbital coefficients and highest occupied molecular orbital (HOMO) and lowest unoccupied molecular orbital (LUMO) energies of **4a** and acrylonitrile used in the FMO analysis.

The stationary points found with MOPAC93 were fully reoptimized using the Gaussian94 suite of programs[11] at the restricted Hartree−Fock (RHF) level of theory, using the split-valence d polarization with diffuse functions 6-31+G*. Harmonic vibrational frequencies were calculated at the RHF/6-31+G* level in order to characterize stationary points (minima and saddle points).

Intrinsic reaction coordinate (IRC) calculations[12] at the RHF/6-31+G* level were performed from the transition states to verify which state connects the two minima points predicted by the transition vector. With the purpose of checking the IRC calculation evolution, a program was designed to capture the energy Hessian of the optimized points from the Gaussian94 output file, to project them upon the subspace orthogonal to the gradient vector, and to diagonalize them.

Experimental Results and Discussion

Synthesis. To explore the reactivity of **3** (X = N), we initially examined the reaction of **3a** with methylpropiolate heated under reflux (6 h) in CH_2Cl_2 in the presence of *N*-ethyldiisopropylamine (Hünig's base), leading to the expected cycloaddition product **9** (36%), which was isolated from a complex reaction mixture (Scheme 2). In sharp contrast to this result, the reaction of **3a** with the typical olefinic dipolarophile, *N*-methylmaleimide in CH_2Cl_2, in the presence of Hünig's base, produced a mixture of the cycloadducts **10** and **11** in 84% yield (2:3), along with traces of the heterobetaine **12**, after 2 h at room temperature. Surprisingly, the cyclocondensation product **12** was obtained as the major component (49%), accompanied by minor amounts of the cycloadduct **10** (16%) after 48 h reflux, as evidenced by NMR (Scheme 3).

The assigned structure of the major regioisomer **11** was established by ^{1}H NMR data on the basis of chemical shifts of the dihydropyridine moiety, which shows well-resolved signals for H_4-H_7. Similarly, the structure of the cycloadduct **10** derived from ^{1}H NMR was identified as the endo-cycloadduct. Coupling constants between H_3

(9) Stewart, J. J. *MOPAC 93.00 Manual*, Fujitsu Limited, Tokyo. Japan, 1993.

(10) (a) Steward, J. J. P. *J. Comput. Chem.* **1989**, *10*, 109. (b) Steward, J. J. P. *J. Comput. Chem.***1989**, *10*, 221.

(11) Frisch, M. J.; Trucks, G. W.; Schlegel, H. B.; Gill, P. M. W.; Johnson, B. G.; Robb, M. A.; Cheeseman, J. R.; Keith, T. A.; Petersson, G. A.; Montgomery, J. A.; Raghavachari, K.; Al-Laham, M. A.; Zakrzewski, V. G.; Ortiz, J. V.; Foresman, J. B.; Peng, C. Y.; Ayala, P. Y.; Wong, M. W.; Andres, J. L.; Replogle, E. S.; Gomperts, R.; Martin, R. L.;. Fox, D. J.; Binkley, J. S.; Defrees, D. J.; Baker, J.; Stewart, J. P.; Head-Gordon, M.; Gonzalez, C.; Pople, J. A. *Gaussian94 (Revision A.1)*, Gaussian, Inc., Pittsburgh, PA, 1995.

(12) (a) Gonzalez, C.; Schlegel, H. B. *J. Chem. Phys.* **1989**, *90*, 2154. (b) Gonzalez, C.; Schlegel, H. B. *J. Phys. Chem.* **1990**, *94*, 5523.

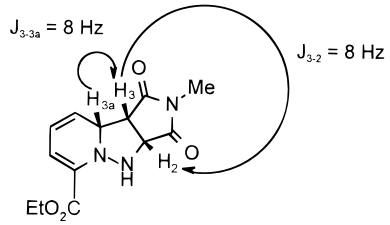

Figure 1. Selected ^{1}H NMR data of cycloadduct **10**.

and H_{3a} (J = 8 Hz), as well as H_3 and H_2 (J = 8 Hz), were consistent with a cis disposition for these hydrogens (Figure 1). Full characterization of **10** and **11** was unambiguously established by irradiation of the protons.

During attempts to characterize **11**, bidimensional TLC experiments (silica gel, EtOAc, MeOH) revealed that the cycloadduct **11** was easily transformed into the heterobetaine **12**. Furthermore, when **11** was isolated and heated in CH_2Cl_2, the heterobetaine **12** was also formed. Under the same conditions, however, the cycloadduct **10** decomposes extensively.

This result prompted us to investigate the reaction of **3a** with different asymmetrical dipolarophiles. Thus, when **3a** was refluxed with acrylonitrile in CH_2Cl_2, for 20 h in the presence of Hünig's base, compound **13a** was the only isolated product (86%), which was subsequently converted into the heterobetaine **14a** in good yield (95%) using 2,3-dichloro-5,6-dicyano-1,4-benzoquinone (DDQ) (Scheme 3). After the initial 15 min, TLC revealed that the reaction mixture contained adducts similar to **10** and **11**, together with heterobetaine **13a**. With longer reflux periods, one of the cycloadducts (highest R_f, similar to **11**) was transformed into **13a**, as observed by bidimensional TLC (silica gel, hexane:EtOAc, 1:1/MeOH).

The scope of the process was tested with different olefinic dipolarophiles (Scheme 4). Thus, in the first series of experiments, **3a** reacted with 2-butenenitrile to produce the dihydro derivative **13b** (60%) as the major product, together with the fully aromatized product **14b** as the minor component (12%). Analogous results were obtained when **3a** was reacted with methyl vinyl ketone in the presence of Hünig's base to produce the expected heterobetaine **13c** (52%) together with **14c** (18%). Furthermore, the heterobetaine **13c** was transformed to **14c** in 71% yield after refluxing for 3 h in acetonitrile. We also tested the reaction of **3a** with crotonaldehyde, allowing access to **13d** (25%) from a complex reaction mixture.

Under the same conditions, when phenyl acrylonitrile and methyl styryl ketone were used as dienophiles, the fully aromatized heterobetaines **14e** and **14f** were obtained. An explanation for these results could be that a phenyl substituent in the 2-position in **14e** and **14f** facilitates the aromatization of the heterobetaine. When **3a** was reacted with phenyl vinyl sulfone under similar conditions, however, the heterobetaine **18** and the cycloadduct **15** were isolated in 30% and 46% yield, respectively (Scheme 4), together with small amounts (4%) of **19**, which bears the benzenesulfonyl substituent. It is noteworthy that this reaction behaves in a manner similar to that with *N*-methylmaleimide, although in this case the cycloadduct **15** is the major component of the reaction mixture. Moreover, we have previously observed that only one of the cycloadducts formed in the cycloaddition process is capable of being converted into the heterobetaine, and thus, we assumed that the formation of **18** and **19** via the corresponding cycloadduct **16** would initially provide the benzenesulfonyl dihydroderivative **17**, which can subsequently be oxidized to give **19** or undergo a β-elimination to yield **18** (Scheme 5).

The structure and stereochemistry of the cycloadduct **15** was assigned initially on the basis of ^{1}H NMR chemical shifts and coupling constants observed for H_3 (ddd, J = 8.3 Hz, J = 5.7 Hz, and J = 2.2 Hz), H_{3a} (ddd, J = 5.7 Hz and J = 4.1 Hz), and $H_{2'}$ (dd, J = 13 Hz and J = 8.3 Hz). A cis relationship between H_3 and $H_{2'}$ in **15** was assigned on the basis of the coupling constants of J = 8.3 Hz between both hydrogens. In the case of

Scheme 3

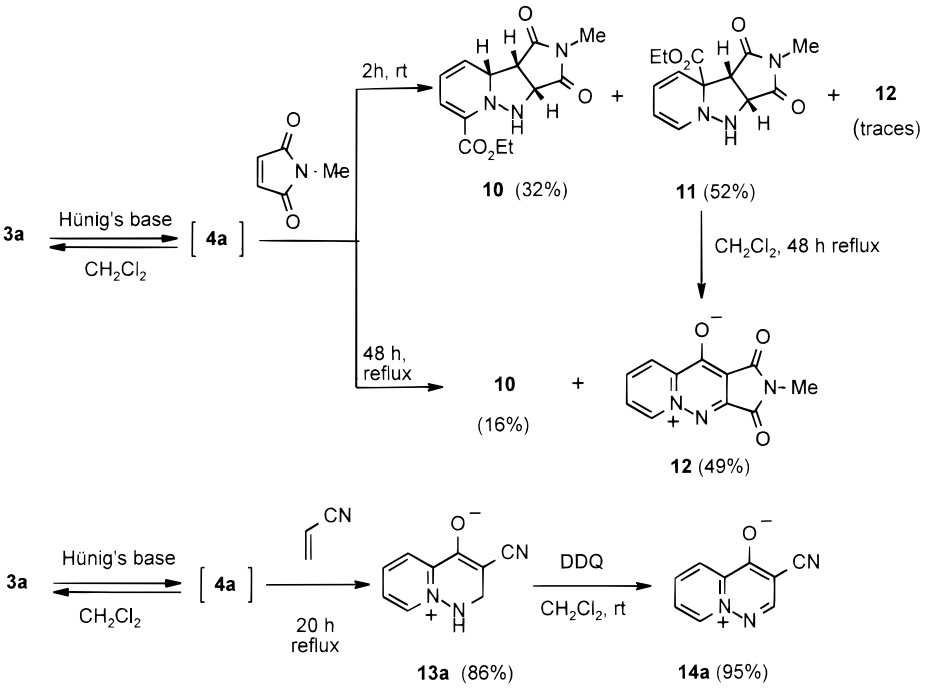

Scheme 4

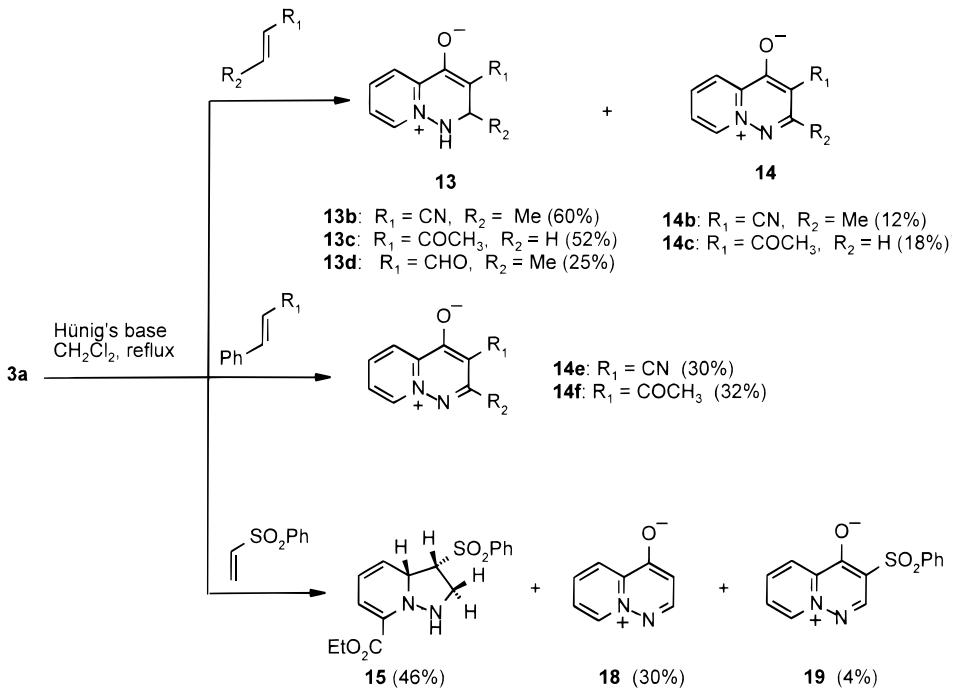

Scheme 5

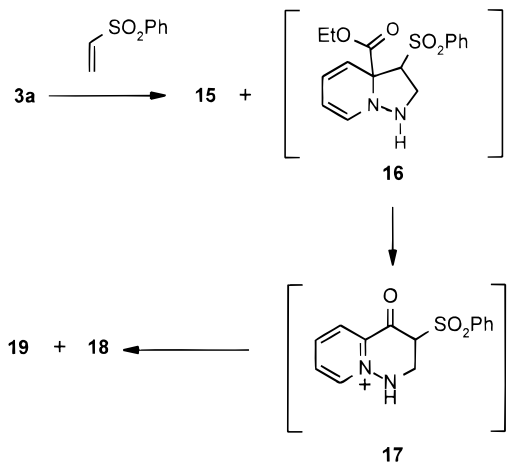

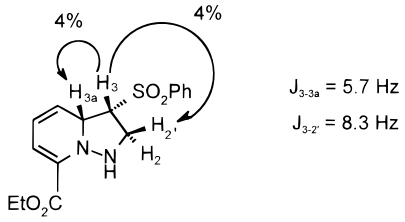

Figure 2. Coupling constants and NOE observed upon irradiation of selected protons in cycloadduct **15**.

the H_3/H_{3a}, coupling constant values (J = 5.7 Hz) were too ambiguous to allow assignment of their relative geometries, and the entire stereostructure was firmly established through NOE difference experiments (Figure 2).

We were also interested in extending the process to alcoxycarbonyl quinolinium and isoquinolinium salts **3b** and **3c**, to obtain novel tricyclic heterobetaines. Thus, the reaction of quinolinium *N*-aminide **4b** with acrylonitrile in CH_2Cl_2, in the presence of Hünig's base produced, after 20 h reflux, a mixture of endo/exo-cycloadducts **20** and **21** (4:1), respectively, in 75% yield, and traces of the heterobetaine **23** (Scheme 6).

In the latter case, although the heterobetaine was only detected by TLC, we assumed its formation via a ring expansion process. Consequently, according to our previous results, we expected that refluxing the mixture of cycloadducts **20** and **21** would result in extensive formation of the heterobetaine **23**. After refluxing in CH_3CN for 20 h, however, the heterobetaine **23** was isolated in only a 4% yield, together with 3-cyanopyrazolo[1,5-*a*]-quinoline **22** in 61% yield (Scheme 6). Analogous behavior was observed from the reaction of isoquinoliniun N-aminide **4c** with acrylonitrile, leading to a mixture of endo/exo products, which under prolonged reflux were transformed into the fully aromatic compound **26**, although in this case the corresponding heterobetaine was not even detected (Scheme 6).

Although the stereochemistry of the major cycloadduct **20** could not be firmly established on the basis of NMR analysis, the observed stereoselectivity might be explained in terms of the transition states coming from the endo and exo approaches. As depicted in Figure 3, the endo approach is clearly favored, because both the steric interaction between the cyano and the ethoxycarbonyl groups and the attractive π interaction working between the heterocyclic system and the cyano group are more favorable in the transition state leading to the endo-cycloadduct. An explanation for the above results (oxidation of the cycloadducts **20**/**21** and **24**/**25** instead of ring expansion) might be related to the aromaticity of these cycloadducts when compared with the nonaromatic cycloadduct **11**, formed in the reaction of **4a** with olefinic dipolarophiles.

These results demonstrate the ability of **4a** to act as a 1,3-dipole toward olefinic dipolarophiles and the subsequent rearrangement of some of the formed cycloadducts to afford the corresponding heterobetaines. To our knowledge, this is the first example of a cycloadduct involved in a ring expansion process leading to the formation of

Scheme 6

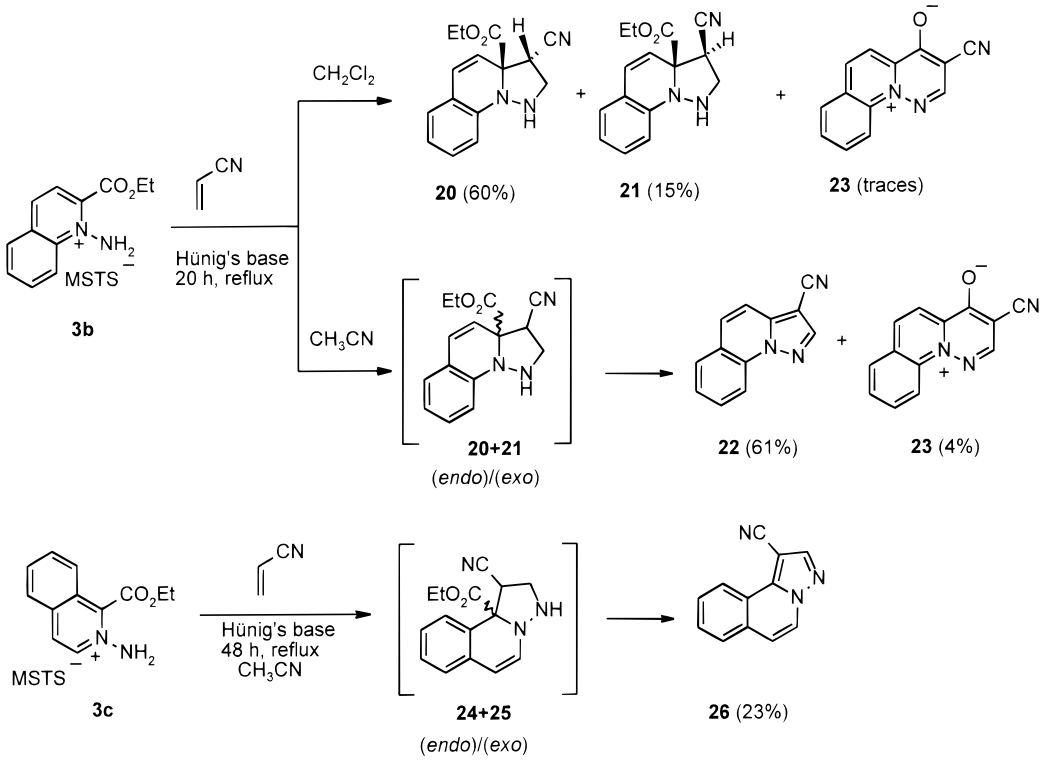

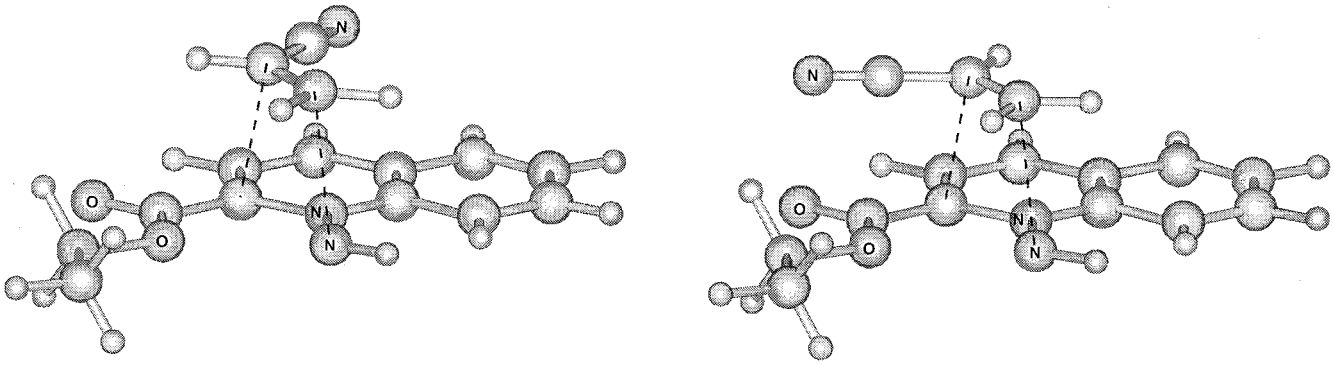

Figure 3. Endo versus exo approach of **4b** and acrylonitrile.

conjugated mesomeric betaines. More than likely, the steric hindrance of one of the regioisomeric cycloadducts would favor its rearrangement toward the more stable heterobetanic system.

Heterobetaine Formation. As the formation of heterobetaines seems to take place through a 1,3-dipolar cycloaddition−ring expansion process, we performed semiempirical and ab initio calculations (i) to confirm that the cycloaddition is initially favored, (ii) to determine whether the cycloaddition proceeds throughout a concerted or stepwise mechanism,[13] and (iii) to examine the mechanism for the arrangement of the cycloadduct. Solving these key issues allowed us to elaborate on a mechanistic model for the formation of pyrido[1,2-*b*]-pyridazinium inert salts, exemplified by the reaction of **4a** and acrylonitrile.

First, a PM3 FMO analysis was performed to determine whether the cycloaddition or the cyclocondensation is initially favored. The resulting HOMO (1,3-dipole)−LUMO (dipolarophile) energy gap is 8.476 eV, whereas the HOMO (dipolarophile)−LUMO (1,3-dipole) energy difference is 10.194 eV. Therefore, reactivity is essentially controlled by the interaction between the HOMO dipole and the LUMO dipolarophile. Clearly, the cycloaddition of the aminide **4a** and acrylonitrile can be characterized as Sustmann's type I classification.[14] Their atomic orbital coefficients for the optimized structures are presented in Figure 4. The largest interaction energy following Fukui's FMO theory[15] is achieved by matching atomic p_z-orbitals of N-7 and C-2 at **4a** with C-3 and C-2 of acrylonitrile, respectively. Furthermore, the cyclocondensation seems a difficult process for two reasons: (a)

(13) For leading references see: (a) Nguyen, M. T.; Chandra, A. K.; Sakai, S.; Morokuma, K. *J. Org. Chem.* **1999**, *64*, 65. (b) Newmann, F.; Lambert, C.; Schleyer, P.v. R. *J. Am. Chem. Soc.* **1998**, *120*, 3357. (c) Houk, K. N.; Beno, B. R.; Nendel, M.; Black, K.; *J. Mol. Struct. (THEOCHEM)* **1997**, *398*−*399*, 169. (d) Houk, K. N.; Yamaguchi, K. *1,3-Dipolar Cycloaddition Chemistry*; Padwa, A., Ed.; John Wiley: New York, 1984; Chapter 13, p 407.

(14) (a) Sustmann, R. *Tetrahedron Lett.* **1971**, 2717. (b) Sustman, R.; Trill, H. *Angew. Chem. Intern. Ed. Engl.* **1972**, *11*, 838. (c) Weingarten, M.; Prein, M.; Price, A. T.; Snyder, J. P.; Padwa, A. *J. Org. Chem.* **1997**, *62*, 2001.

(15) (a) Fukui, K.; Fujimoto, H. *Bull. Chem. Soc. Jpn.* **1968**, *41*, 1989. (b) Fujimoto, H.; Yamabe, S.; Fukui, K. *Bull. Chem. Soc. Jpn.* **1971**, *44*, 2936.

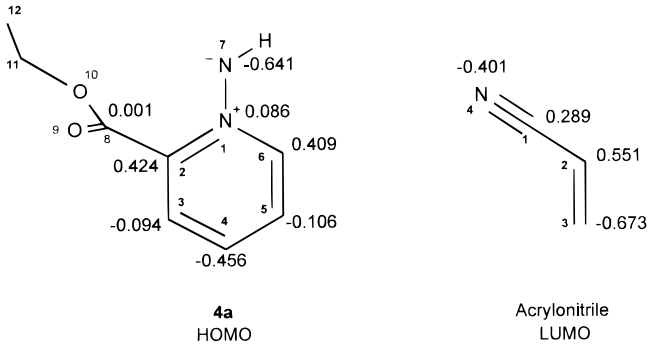

Figure 4. Frontier orbital coefficients which control the cycloaddition of **4a** and acrylonitrile.

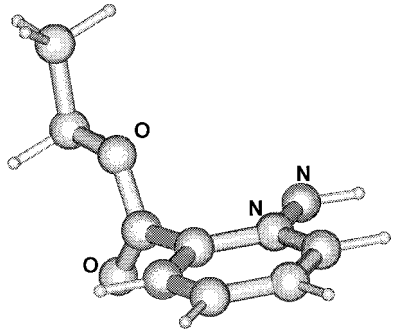

Figure 5. View of **4a** showing orientation of carbonyl group and pyridinium ring.

because of the low HOMO electronic population over the carbonylic carbon (Figure 4) and (b) because the orientation of the carbonyl group is perpendicular to the pyridinium ring and, thus, not suitable to reach the maximum *p*-orbital overlap (Figure 5). The conformation of the carbonyl group, coplanar to the ring, is not an energy minimum; thus, cycloaddition is the predominant reaction path. This conclusion is consistent with experimental results, where both cycloadducts were either isolated or observed by means of TLC at the beginning of the reaction.

Huisgen et al.[16] described a cycloaddition reaction between a thiocarbonyl ylide and dimethyl dicyano fumarate in which a zwitterionic intermediate is involved in a two-step reaction mechanism, instead of going through a concerted path, as in most cycloadditions. The replacement of the dipolarophile by dimethyl fumarate is sufficient for the concerted pathway to be predominant. There are two causes for this finding: (a) the interaction HOMO (1,3-dipole)−LUMO (dipolarophile) is strongly dominant relative to the alternative HOMO−LUMO interaction, and (b) the steric effect due to the substituents of the 1,3-dipole. We calculated the HOMO (1,3-dipole)−LUMO (dipolarophile) energy gap at PM3/RHF, to be 4.244 eV greater than the HOMO (dipolarophile)−LUMO (1,3-dipole) one, using dimethyl dicyano fumarate as a dipolarophile, in contrast to an energy difference of 3.175 eV with dimethyl fumarate. In the present case, this energy separation is only 1.718 eV and this, together with a smaller steric repulsion, led us to assume a predominant concerted mechanism for the cycloaddition reaction.

On the other hand, bidimensional TLC experiments and heating of the initial cycloadducts revealed that one of the cycloadducts was easily transformed into a heterobetaine. Consequently, there is a reaction path that would lead to the heterobetaine from the cycloadduct.

A careful study of PES was performed, to determine the subsequent reaction steps and to confirm the results of the PM3 FMO theory. The theoretical model to explain the reaction path from the cycloadduct to heterobetaine (see Scheme 7), assuming that the heterobetaine comes from the tetrahedral intermediate (**INT 3**), was successful. From this intermediate (Figure 6), the heterobetaine **13a** was obtained by losing ethanol. From **INT 3** we initiated the study of the pathway toward the reactants. The transition state **TS 3**, involved in the breaking of the bond between C-3 and C-4, was obtained by means of a scan along this bond, and its optimized geometry is shown in Figure 6 with its interatomic distances. An intrinsic reaction coordinate (IRC) calculation from transition state **TS 3** was performed in the direction of the reactants. The study of the number of energy Hessian negative eigenvalues, the force vector orientation relative to energy Hessian eigenvectors, and the energy gradient norm along the curve allowed us to conclude that it does not pass through any transition states or any bifurcation points prior to production of the two products.[17] Therefore, the IRC calculation reveals a pathway without a stationary point between transition state **TS 3** and the cycloadduct (**INT 2**) after passing through 210 optimized points. This result is not predictable with regard to the transition vector, due to a great variation in curve direction, which takes place at about the middle of the path and without passing through a stationary point. This behavior is due to the stretching of bond C3−C4, which simultaneously begins to weaken as the bond C-3−C-4a starts to strengthen in this curve point.

A scan was performed from a point placed in the abovementioned IRC curve portion. The dihedral angle N-9, N-1, C-2, C-3 was varied so that C-3 moved away from the pyridinium ring. By means of this calculation, a maximum energy point was found with one imaginary frequency. After the optimization, the geometry of **TS 2** presented in Figure 6 was obtained. Another IRC calculation was performed toward both directions. In the forward IRC calculation, the minimum energy reaction intermediate, **INT 1**, was obtained. In the opposite direction, the IRC curve arrived at geometries similar to those in the last portion of the IRC curve, which connects transition state **TS 3** and cycloadduct (**INT 2**). The above results indicate that there are two reaction paths that converge to the same valley. This implies the existence of a bifurcation prior to the two transition states, **TS 2** and **TS 3**. At the IRC points preceding the bifurcation point, the energy Hessian projected upon the subspace perpendicular to the gradient vector has no negative eigenvalue, which implies that the IRC curve does not pass through a transition state before reaching the bifurcation point. On the other hand, at the second step (**INT 1→INT 2**) there is no energy barrier due to the formation of the C-3−C-4a bond via a zwitterionic intermediate but only by passing through an eclipsed conformation of the dihedral angle N-9, N-1, C-2, C-3.

A transition state **TS 1** corresponding to a concerted cycloaddition was also found. Thus, two pathways com-

(16) Huisgen, R.; Mloston, G.; Langhals, E. *J. Am. Chem. Soc.* **1986**, *108*, 6401.

(17) Valtazanos P.; Ruedenberg K. *Theor. Chim. Acta* **1986**, *69*, 281.

Scheme 7

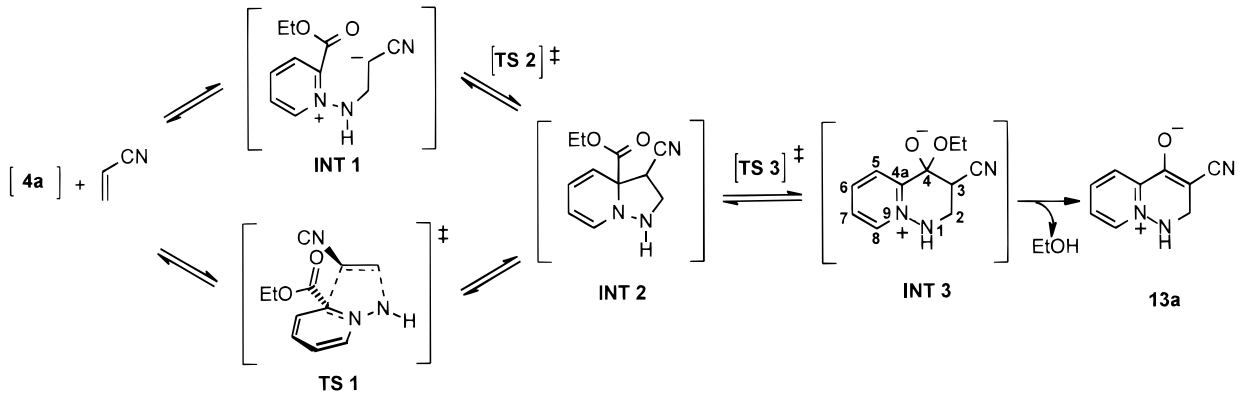

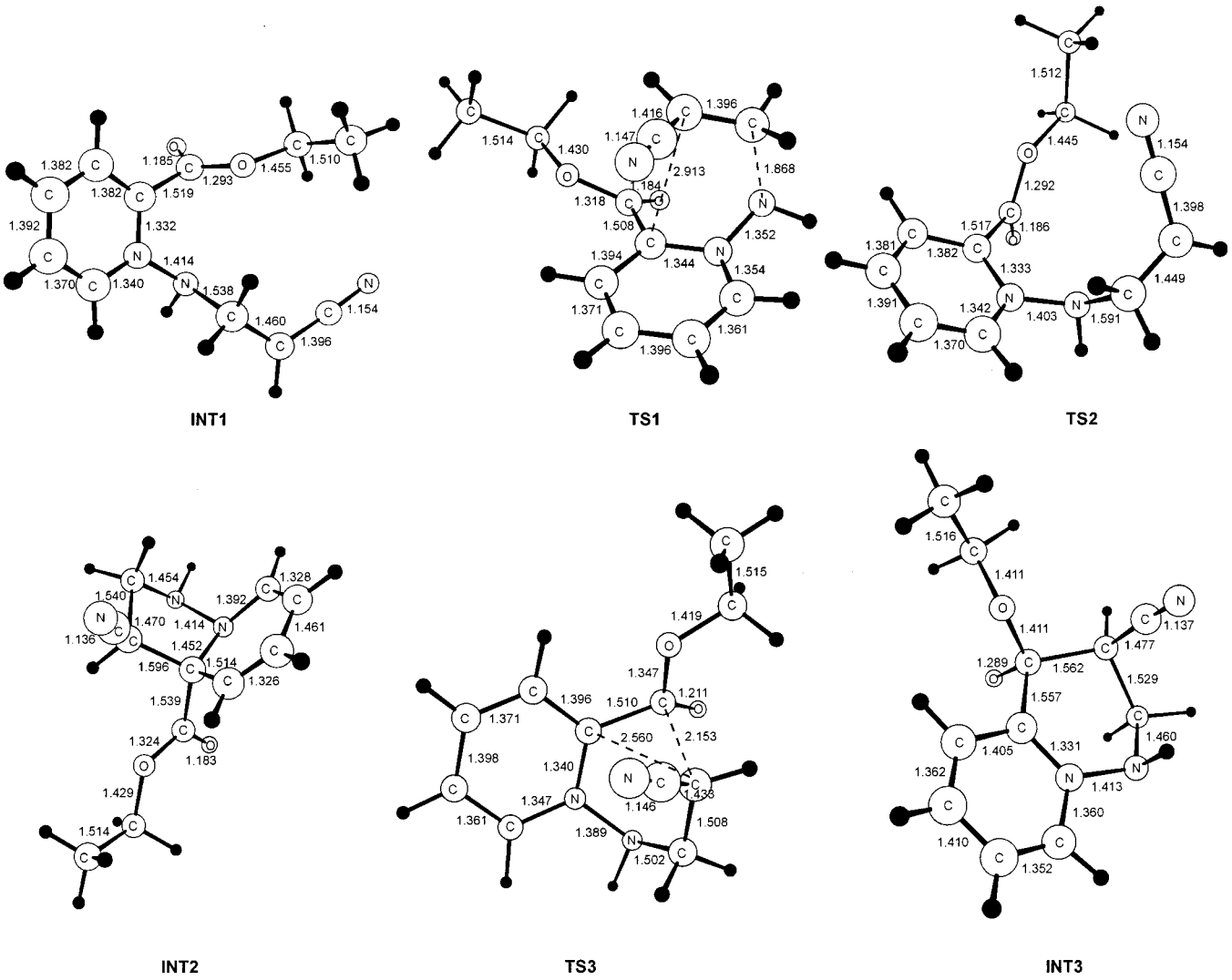

Figure 6. Geometries of stationary points. The distances between heavy atoms are in Angstroms.

pete to reach the cycloaddition, a concerted reaction through a single transition state **TS 1** and a two-step mechanism through a zwitterionic intermediate **INT 1**. A zwitterionic intermediate has already been described[6,18] and proposed as a predominant pathway in other cycloaddition reactions, in which the dipolarophile has three or four electron-withdrawing groups or, alternatively, groups able to stabilize a negative charge. This does not take place in the present case, and it is not expected that a predominant cycloaddition occurs *via* a zwitterionic intermediate. The theoretical results support this hypothesis. The transition state **TS 1** energy is 1.00 kcal/mol lower in energy than the intermediate **INT 1**, and consequently, it is still lower than the energy of the transition state that conducts to the intermediate from the reactants. According to the PM3 FMO, the concerted pathway is more advantageous.

(18) (a) Huisgen R.; Langhals, E.; Noth, H. *J. Org. Chem.* **1990**, *55*, 1412. (b) Quast, H.; Regnat, D.; Peters, K.; Schnering, H. G. *Angew. Chem., Int. Ed. Engl.* **1990**, 29.

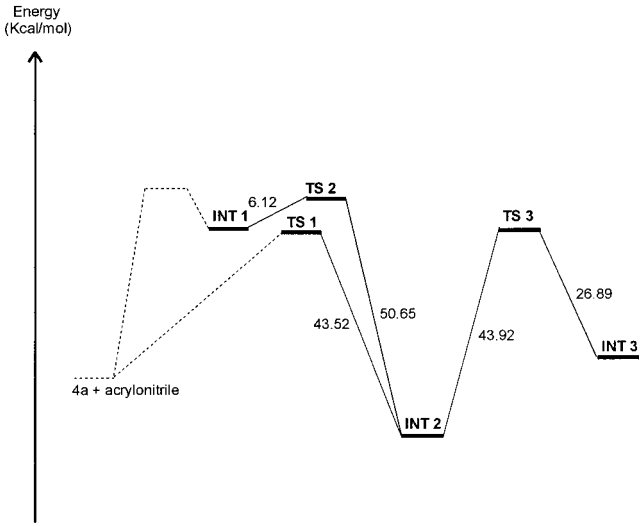

Figure 7. Energetic diagram of the reaction mechanism. The dashed line correspond to the supposed energetic barrier arising by forming N-1−C-2 bond.

The energetic diagram of the reaction mechanism (Scheme 7) deduced from these calculations is shown in Figure 7. The main steps are summarized below:

Step 1 is a cycloaddition, which fundamentally takes place through a concerted mechanism. There is an alternative two-step path via a zwitterionic intermediate, which is energetically less advantageous. In the latter case, the bond between N-2 of **4a** and C-2 of acrylonitrile is formed, and a zwitterionic intermediate (**INT 1**) is obtained. Then, it passes through an eclipsed conformation to form the second bond, and cycloadduct (**INT 2**) is formed.

In step 2, reversion from the cycloadduct (**INT 2**) conducts to a bifurcation point from which two valleys emerge. The reaction goes on either toward the transition state **TS 2** and subsequently toward the intermediate **INT 1** returning to the first step described or toward the transition state **TS 3** and then toward tetrahedral intermediate (**INT 3**), the last alternative bearing the lower energy barrier. From this intermediate, the heterobetaine **13a** is obtained by elimination of ethanol and oxidation.

This pathway competes with cycloadduct reversion through **TS 1**, but elimination of ethanol and heterobetaine precipitation irreversibly displace the whole process.

It is possible to generalize this model to the other studied dipolarophiles (except methylpropiolate), which behave in a similar way when reacted with **4a**. When methylpropiolate is used, ring oxidation is more kinetically favored than ring expansion.

Conclusions

The *N*-aminide **4a** functions as a 1,3-dipole with olefinic dipolarophiles, leading to the corresponding cycloadducts as a previous step to heterobetaine formation. Depending on the regioisomeric nature, one of the cycloadducts formed undergoes a ring expansion process, which leads to a pyrido[1,2-*b*]pyridazinium inner salt. The cycloaddition and the cyclocondensation do not rival each other, but the former is a step prior to the expansion of the pyrazolidine ring to the heterobetaine.

This conclusion is supported by PM3 FMO analysis and ab initio calculations to explore the potential energy surface (IRC). Additionally, two reaction pathways, concerted and stepwise, toward the cycloadduct (**INT 2**) have been found using this methodology. The concerted reaction is energetically more advantageous as determined by the ab initio results.

The *N*-aminide **4a** also reacts as a 1,3-dipole with acetylenic compounds to afford the corresponding cycloadducts, which are the only isolated products from the reaction with methyl propiolate. The initial formation in this case of a partially oxidized cycloadduct likely explains its different behavior toward the rearrangement process. Cycloadducts from quinolinium and isoquinolinium *N*-aminides are also more easily oxidized, precluding the expansion ring process.

Experimental Section

General. Melting points are uncorrected. Mass spectra were determined at an ionizing voltage of 70 eV. The ^{1}H and ^{13}C NMR were collected on Varian instruments. Column chromatogaphy was performed on silica gel 60 (230−400 mesh). Mesitylenesulfonate of 1-amino-2-ethoxycarbonyl pyridinium **3a**−**c** was obtained by previously described methods.[6]

Pyrazolo[1,5-*a*]pyridine-3,7-dicarboxylic Acid 7-Ethyl 3-Methyl Diester (9). To a solution containing 0.37 g (1 mmol) of the salt **3a** in dry CH_2Cl_2 (10 mL) were added methyl propiolate (0.1 mL, 1.1 mmol) and *N*-ethyldiisopropylamine, (0.35 mL, 2 mmol), and the reaction mixture was refluxed for 6 h. The solvent was then evaporated under reduced pressure and the residue was purified by chromatography using hexane/EtOAc (8:2) as eluent, to give 94 mg (36%) of **9** as a pale powdery solid: mp 81−82 °C; IR (KBr) 1735, 1699, 1631, 1536, 1372, 1240, 1206, 1144 cm^{-1}; ^{1}H NMR ($CDCl_3$, 300 MHz) δ 8.53 (s, 1H), 8.41 (dd, 1H, J = 8.8, 1.5 Hz), 7.62 (dd, 1H, J = 7.1, 1.5 Hz), 7.48−7.42 (m, 1H), 4.54 (q, 2H, J = 7.1 Hz), 3. 93 (s, 3H), 1.46 (t, 3H, J = 7.1 Hz);^{13}C NMR ($CDCl_3$, 50 MHz) δ 163.6, 160.6, 144.9, 141.9, 130.8, 125.9, 122.7, 118.0, 112.8, 62.5, 51.3, 14.2. Anal. Calcd for $C_{12}H_{12}N_2O_4$: C, 58.06; H, 4.87; N, 11.28. Found: C, 57.75; H, 5.18; N, 11.19.

2,3-(*N*-Methyldicarboximido)-2,3-dihydro-1*H*-pyrazolo-[1,5-*a*]pyridine-3a-carboxylic Acid Ethyl Ester (11) and 2,3-(*N*-Methyldicarboximido)-1,2,3,3a-tetrahydropyrazolo-[1,5-*a*]-pyridine-7-carboxylic Acid Ethyl Ester (10). To a solution of the salt **3a** (0.37 g, 1 mmol) in dry CH_2Cl_2 (10 mL) were added *N*-methylmaleimide (0.12 g, 1.1 mmol) and *N*-ethyldiisopropylamine (2 mmol). The mixture was stirred for 2 h. The residue was purified by chromatography (EtOAc). The cycloadduct **11** (0.14 g, 52%) was eluted first and isolated as a pale yellow solid. The adduct **10** (88 mg, 32%) was obtained as yellow oil.

11: ^{1}H NMR ($CDCl_3$, 500 MHz) δ 6.18 (dt, 1H, J = 7.5, 1.0 Hz), 5.99 (ddd, 1H, J = 10.0, 6.0, 1.0 Hz), 5.69 (dt, 1H, J = 10.0, 1.0 Hz), 5.07 (d, 1H, J = 6.5 Hz, −NH), 4.72 (ddd, 1H, J = 7.5, 6.0, 1.0 Hz), 4.30−4.20 (m, 2H), 4.19 (dd, 1H, J = 7.5, 6.5 Hz), 3.78 (d, 1H, J = 7.5 Hz), 2.84 (s, 3H), 1.31 (t, 3H, J = 7.0 Hz).

10: ^{1}H NMR ($CDCl_3$, 500 MHz) δ 5.98 (dd, 1H, J = 10.0, 5.6 Hz), 5.93 (ddd, 1H, J = 10.0, 4.4, 1.5 Hz), 5.50 (dd, 1H, J = 5.6, 1.5 Hz), 5.21 (d, 1H, J = 5.0 Hz, −NH), 4.42 (dd, 1H, J = 8.0, 4.4 Hz), 4.29−4.16 (m, 3H), 3.50 (t, 1H, J = 8.0 Hz), 2.85 (s, 3H), 1.29 (t, 3H, J = 7.0 Hz).

3-Benzenesulfonyl-1,2,3,3a-tetrahydropyrazolo[1,5-*a*]-pyridine-7-carboxylic Acid Ethyl Ester (15). To a stirred solution containing the salt **3a** as iodide (0.29 g, 1 mmol) in CH_2Cl_2 (15 mL) were added phenylvinyl sulfone (0.12 g, 1.1 mmol) and K_2CO_3 (2 mmol), and the reaction was refluxed for 4 h. Then, the inorganic residue was filtered off and the liquid was concentrated to dryness. The residue was purified by chromatography (hexane/EtOAc, 1:1) to give 0.15 mg of **15** (46%) as yellow oil: ^{1}H NMR ($CDCl_3$, 500 MHz) δ 7.92−7.87

(m, 2H), 7.75−7.68 (m, 1H), 7.65−7.58 (m, 2H), 5.83 (ddd, 1H, J = 9.7, 6.0, 1.3 Hz), 5.62 (dd, 1H, J = 6.0, 1.2 Hz), 5.25 (ddd, 1H, J = 9.7, 3.9, 1.2 Hz), 4.78 (ddd, 1H, J = 5.7, 4.0, 1.5 Hz), 4.42−4.32 (m, 1H, −NH), 4.30−4.10 (m, 2H), 3.76 (ddd, 1H, J = 8.3, 5.7, 2.2 Hz), 3.52 (dd, 1H, J = 13.0, 2.0 Hz), 2.86 (dd, 1H, J = 13.0, 8.3 Hz); NOE exp: 3.76, H_3-H_{3a} (4%), $-H_{2'}$ (4%); 3.52, $H_2-H_{2'}$ (11%); 2.86 $H_{2'}$-H_2 (10.5%), $-H_3$ (12.5%); ^{13}C NMR ($CDCl_3$, 125 MHz) δ 164.9, 140.0, 138.7, 138.0, 134.3, 129.7, 128.4, 122.7, 121.9, 107.3, 62.1, 61.2, 46.7, 14.1.

Synthesis of Heterobetaines. General Procedure. To a solution of the salt **3a** (0.36 g, 1 mmol) and the appropriate dipolarophile (1.1 mmol) in dry CH_2Cl_2 (10 mL) was added *N*-ethyldiisopropylamine (0.35 mL, 2 mmol) dropwise. The reaction mixture was refluxed over 20−48 h, as indicated.

4-Hydroxy-2,3-(*N*-methyldicarboximido)pyrido[1,2-*b*]-pyridazinium Inner Salt (12). Method A. Starting from *N*-methylmaleimide and refluxing the mixture for 48 h, the precipitate formed was isolated by filtration. Recrystallization from DMF yielded 0.11 g (49%) of **12** as a pale yellow solid. **Method B**. A solution of the cycloadduct **11** (0.14 g, 0.5 mmol) in CH_2Cl_2 (5 mL) was refluxed for 48 h. The resulting precipitate was isolated by filtration, to give 53 mg (46%) of **12**: mp >300 °C (DMF); IR (KBr) 1710, 1617, 1589, 1537, 1437, 1375 cm^{-1}; ^{1}H NMR (DMSO-d_6, 300 MHz) δ 9.39 (d, 1H, J = 6.6 Hz), 8.71 (d, 1H, J = 7.7 Hz), 8.42 (t, 1H, J = 7.7 Hz), 8.19−8.11 (m, 1H), 2.98 (s, 3H); ^{13}C NMR (DMSO-d_6, 50 MHz) δ 165.2, 164.8, 161.1, 154.5, 147.6, 146.8, 142.3, 139.4, 127.4, 124.4, 23.5; MS (*m*/*z*) 229 (M^+, 55), 106 (55), 78 (100). Anal. Calcd for $C_{11}H_7N_3O_4$: C, 57.65; H, 3.08; N, 18.33. Found: C, 57.59; H, 3.29; N, 17.98.

3-Cyano-4-hydroxy-1,2-dihydropyrido[1,2-*b*]pyridazinium Inner Salt (13a) and 3-Cyano-4-hydroxypyrido[1,2-*b*]pyridazinium Inner Salt (14a). From acrylonitrile (1.1 mmol) and refluxing the mixture for 20 h, the resulting precipitate was isolated by filtration to afford 0.15 g (86%) of **13a** as an orange solid: mp 194−195 °C (CH_3CN/DMF); IR (KBr) 3060, 2839, 2173, 1576, 1551, 1476, 1392, 1263 cm^{-1}; ^{1}H NMR (DMSO-d_6, 300 MHz) δ 8.65 (d, 1H, J = 6.6 Hz), 8.46 (sa, 1H), 8.33−8.20 (m, 2H), 7.86−7.78 (m, 1H), 3.97 (s, 2H); ^{13}C NMR (DMSO-d_6, 50 MHz) δ 161.1, 147.0, 141.6, 139.3, 126.0, 123.6, 122.5, 66.7, 44.3; MS (*m*/*z*) 173 (M^+, 10), 171 (81), 78 (100). Anal. Calcd for $C_9H_7N_3O$: C, 62.42; H, 4.07; N, 24.26. Found: C, 62.32; H, 4.13 N, 23.96.

14a. To a suspension of **13a** (1 mmol) in dry CH_2Cl_2 (10 mL) was added DDQ (0.22 g, 1 mmol), and the reaction mixture was stirred for 2 h at room temperature. After evaporation of the solvent the residue was purified by chromatography on silica gel using acetone as eluent to give 0.16 g (95%) of **14a** as white solid: mp 278−280 °C (CH_3CN); IR (KBr) 2215, 1636, 1606, 1577, 1533, 1467, 1329, 1285 cm^{-1}; ^{1}H NMR (DMSO-d_6, 300 MHz) δ 9.18 (d, 1H, J = 7.0 Hz), 8.76 (s, 1H), 8.60 (dd, 1H, J = 8.1, 1.5 Hz), 8.38−8.30 (m, 1H), 8.12−8.06 (m, 1H); ^{13}C NMR (DMSO-d_6, 50 MHz) δ 166.3, 152.9, 143.5, 140.4, 138.3, 127.1, 123.4, 116.8, 89.1; MS (*m*/*z*) 171 (M^+, 100), 143 (95), 116 (63). Anal. Calcd for $C_9H_5N_3O$: C, 63.16; H, 2.94; N, 24.55. Found: C, 63.01; H, 3.05; N, 24.18.

3-Cyano-4-hydroxy-2-methyl-1,2-dihydropyrido[1,2-*b*]-pyridazinium inner salt (13b) and 3-cyano-4-hydroxy-2-methylpyrido[1,2-*b*]pyridazinium inner salt (14b) were obtained from 2-butenenitrile (1.1 mmol) by refuxing the mixture for 20 h. The yellow precipitate was filtered off to give 0.11 g (60%) of **13b**: mp 226−227 °C (CH_3CN); IR (KBr) 3079, 3035, 2167, 1562, 1530, 1398 cm^{-1}; ^{1}H NMR (DMSO-d_6, 300 MHz) δ 8.63 (d, 1H, J = 6.2 Hz), 8.54 (bs, 1H), 8.30−8.19 (m, 2H), 7.88−7.80 (m, 1H), 4.32 (q, 1H, J = 6.2 Hz), 1.24 (d, 3H, J = 6.6 Hz). Anal. Calcd for $C_{10}H_9N_3O$: C, 64.16; H, 4.85; N, 22.45. Found: C, 64.01; H, 4.76; N, 22.30. The filtrate was concentrated and the residue was chromatographed (acetone). **14b** was obtained (22 mg, 12%) as pale yellow solid: mp >300 °C; IR (KBr) 3415, 2209, 1642, 1596, 1521 cm^{-1}; ^{1}H NMR ($CDCl_3$, 300 MHz) δ 8.79−8.74 (m, 2H), 8.09−8.02 (m, 1H), 7.83−7.75 (m, 1H), 2.60 (s, 3H). Anal. Calcd for $C_{10}H_7N_3O$: C, 64.86; H, 3.81; N, 22.69. Found: C, 64.75; H, 3.56; N, 22.52.

3-Acetyl-4-hydroxy-1,2-dihydropyrido[1,2-*b*]pyridazinium inner salt (13c) and 3-acetyl-4-hydroxypyrido[1,2-*b*]pyridazinium inner salt (14c) were obtained from 3-buten-2-one (1.1 mmol) by refluxing the mixture for 20 h. The precipitate was isolated by filtration to give 99 mg (52%) of **13c** as a yellow solid: mp 190−192 °C (CH_3CN); IR (KBr) 3027, 1568, 1529, 1431, 1273 cm^{-1}; ^{1}H NMR (DMSO-d_6, 300 MHz) δ 8.64−8.56 (m, 2H), 8.36−8.31 (m, 1H), 8.25−8.18 (m, 1H), 7.85−7.77 (m, 1H), 4.08−4.05 (m, 2H), 2.34 (s, 3H); ^{13}C NMR (DMSO-d_6, 50 MHz) δ 190.2, 161.4, 148.0, 137.2, 126.3, 124.9, 101.8, 44.3, 29.7. Anal. Calcd for $C_{10}H_{10}N_2O_2$: C, 63.15; H, 5.30; N, 14.73. Found: C, 62.92; H, 5.28; N 14.55. The filtrate was concentrated and the residue was chromatographed (acetone) to give 34 mg (18%) of **14c** as a pale yellow solid: mp 214−215 °C; IR (KBr) 1652, 1596, 1524, 1461, 1364, 1275; ^{1}H NMR ($CDCl_3$, 300 MHz) δ 8.97 (s, 1H), 8.93−8.80 (m, 2H), 8.13−8.03 (m, 1H), 7.83−7.74 (m, 1H), 2.77 (s, 3H). Anal. Calcd for $C_{10}H_8N_2O_2$: C, 63.82; H, 4.28; N, 14.88. Found: C, 63.79; H, 4.02; N 14.65. The crude product **13c** could be directly transformed into **14c** quite effectively by refluxing 19 mg (0.1 mmol) of **13c** in acetonitrile for 3 h. Silica gel chromatography using acetone afforded 13 mg (71% yield) of **14c**.

3-Formyl-4-hydroxy-2-methyl-1,2-dihydropyrido[1,2-*b*]-pyridazinium Inner Salt (13d). Following the general procedure, from crotonaldehyde (0.092 mL, 1.1 mmol) by refluxing the mixture for 4 h, the resulting precipitate was filtered off, yielding 48 mg (25%) of **13d** as orange solid: mp 188−189 °C (CH_3CN); IR (KBr) 3082, 3028, 1605, 1565, 1527, 1434, 1349, 1256 cm^{-1}; ^{1}H NMR (DMSO-d_6, 300 MHz) δ 9.58 (s, 1H), 8.86 (s, 1H), 8.65 (d, 1H, J = 6.6 Hz), 8.35−8.20 (m, 2H), 7.95−7.87 (m, 1H), 4.43 (q, 1H, J = 6.6 Hz), 1.02 (d, 3H, J = 6.6 Hz); ^{13}C NMR (DMSO-d_6, 50 MHz) δ 180.8, 163.3, 146.0, 140.2, 137.8, 127.4, 124.3, 109.6, 48.2, 19.7. Anal. Calcd for $C_{10}H_{10}N_2O_2$: C, 63.14; H, 5.30; N, 14.73. Found: C, 63.49; H, 5.37; N 14.98.

3-Cyano-4-hydroxy-2-phenylpyrido[1,2-*b*]pyridazinium Inner Salt (14e). Starting from 3-phenylacrylonitrile, refluxing the mixture 20 h and purification of the crude product by chromatography with EtOAc/acetone (9:1) gave 74 mg (30%) of **14e** as an orange solid: mp 182−184 °C (CH_3CN); IR (KBr) 2212, 1639, 1604, 1505, 1459, 1438, 1281, 1113 cm^{-1}; ^{1}H NMR (DMSO-d_6, 300 MHz) δ 9.22 (d, 1H, J = 6.6 Hz), 8.63−8.59 (m, 1H), 8.38−8.32 (m, 1H), 8.15−8.09 (m, 1H), 7.80−7.75 (m, 2H), 7.60−7.54 (m, 3H); MS (*m*/*z*) 247 (M^+, 46), 219 (15), 78 (100). Anal. Calcd for $C_{15}H_9N_3O$: C, 72.87; H, 3.67; N, 16.99. Found: C, 73.07; H, 3.86; N, 16.60.

3-Acetyl-4-hydroxy-2-phenylpyrido[1,2-*b*]pyridazinium inner salt (14f) was obtained from 4-phenyl-3-buten-2-one (3 mmol) by refluxing the mixture for 20 h. Purification of the crude product by chromatography (EtOAc/acetone, 9:1) yielded 84 mg (32%) of **14f** as pale brown solid: mp 64−66 °C; IR (KBr) 1691, 1569, 1498, 1461, 1426, 1130 cm^{-1}; ^{1}H NMR ($CDCl_3$, 300 MHz) δ 9.12 (d, 1H, J = 6.8 Hz), 8.61 (d, 1H, J = 8.3 Hz), 8.24−8.18 (m, 1H), 8.06−7.97 (m, 1H), 7.48−7.40 (m, 5H), 2.52 (s, 3H); MS (*m*/*z*) 229 (M^+, 34), 249 (52), 78 (100). Anal. Calcd for $C_{16}H_{12}N_2O_2$: C, 72.72; H, 4.58; N, 10.60. Found: C, 72.35; H, 4.67; N, 10.20.

4-Hydroxypyrido[1,2-*b*]pyridazinium Inner Salt (18) and 3-Benzenesulfonyl-4-hydroxypyrido[1,2-*b*]pyridazinium Inner Salt (19). A mixture of the salt **3a** (0.29 g, 1 mmol) as iodide, phenylvinyl sulfone (0.18 g, 1.1 mmol), and K_2CO_3 (0.28 g, 2 mmol) in dry CH_2Cl_2 (10 mL) was refluxed for 4 h. Purification of the crude product by chromatography (acetone) yielded 44 mg (30%) of **18** as a pale yellow solid: mp 127−128 °C; IR (KBr) 1591, 1508, 1438, 1257;^{1}H NMR ($CDCl_3$, 300 MHz) δ 8.77−8.73 (m, 2H), 8.29 (d, 1H, J = 6.6 Hz), 7.90−7.83 (m, 1H), 7.66−7.59 (m, 1H), 6.52 (d, 1H, J = 7.0 Hz). MS (*m*/*z*) 146 (M^+, 100), 118 (93), 78 (61); ^{13}C NMR ($CDCl_3$, 125 MHz) δ 167.7, 151.1, 145.6, 137.7, 132.3, 124.3, 123.8, 109.1. Anal. Calcd for $C_8H_6N_2O$: C, 65.75; H, 4.14; N, 19.17. Found: C, 65.57; H, 4.01; N, 18.92. Chromatography in EtOAc/acetone 8:2 yielded 11 mg (4%) of **19** as white solid: mp 242−244 °C; IR (KBr) 1637, 1612, 1302, 1282, 1139 cm^{-1}; ^{1}H NMR ($CDCl_3$, 300 MHz) δ 9.00 (s, 1H), 8.85 (d, 1H, J = 6.2 Hz), 8.81−8.76 (m, 1H), 8.23−8.18 (m, 2H), 8.10−8.03 (m, 1H), 7.85−7.78 (m, 1H), 7.61−7.47 (m, 3H). Anal. Calcd for $C_{14}H_{10}N_2O_3S$: C, 58.73; H, 3.52; N,9.78. Found: C, 58.40; H, 3.31; N, 9.56.

Reaction of 2-Ethoxycarbonylquinolinium *N*-Aminide with Acrylonitrile. Method A. Synthesis of 3α-Cyano-2,3-dihydro-1*H*-pyrazolo[1,5-*a*]quinoline-3a*β*-carboxylic Acid Ethyl Ester (20) and 3α-Cyano-2,3-dihydro-1*H*-pyrazolo-[1,5-*a*]quinoline-3aα-carboxylic Acid Ethyl Ester (21). To a solution of 1-amino-2-ethoxycarbonylquinolinium mesitylensulfonate **3b** (0.42 g, 1 mmol) and acrylonitrile (0.075 mL, 1.1 mmol) in dry CH_2Cl_2 (10 mL) was added *N*-ethyldiisopropylamine (0.35 mL, 2 mmol) dropwise. The reaction mixture was refluxed for 20 h, the solvent removed, and the residue chromatographed on silica gel (hexane/EtOAc 9:1 as eluent). **21** (0.040 g, 15%) was eluted first and isolated as a yellow oil. **20** (0.161 g, 60%) was obtained as a white solid.

21: ^{1}H NMR ($CDCl_3$, 300 MHz) δ 7.37 (d, 1H, J = 8.1 Hz), 7.23−7.16 (m, 1H), 6.97 (dd, 1H, J = 7.4, 1.5 Hz), 6.80 (td, 1H, J = 7.4, 1.2 Hz), 6.52 (d, 1H, J = 10.1 Hz), 6.20 (d, 1H, J = 10.1 Hz), 5.20−5.10 (m, 1H), 4.44−4.26 (m, 2H), 3.39−3.29 (m, 2H), 3.17−3.04 (m, 1H), 1.39 (t, 3H, J = 7.1 Hz); ^{13}C NMR ($CDCl_3$, 75 MHz) δ 169.4, 142.6, 130.3, 127.1, 126.6, 120.5, 118.9, 118.4, 117.8, 114.8, 74.3, 62.8, 48.2, 44.2, 14.1.

20: ^{1}H NMR ($CDCl_3$, 300 MHz) δ 7.33 (d, 1H, J = 8.2 Hz), 7.19 (ddd, 1H, J = 8.2, 7.5, 1.5 Hz), 7.05 (dd, 1H, J = 7.5, 1.5 Hz), 6.80 (td, 1H, J = 7.5, 1.5 Hz), 6.72 (d, 1H, J = 10.1 Hz), 5.93 (d, 1H, J = 10.1 Hz), 4.44 (dd, 1H, J = 12.0, 5.1 Hz), 4.25 (q, 2H, J = 7.1 Hz), 3.84 (dd, 1H, J = 8.8, 7.7 Hz), 3.55 (ddd, 1H, J = 11.7, 8.8, 5.1 Hz), 2.87 (ddd, J = 12.0, 11.7, 8.8 Hz), 1.32 (t, 3H, J = 7.1 Hz); ^{13}C NMR ($CDCl_3$, 50 MHz) δ 170.7, 142.06, 130.2, 128.4, 127.5, 120.2, 119.0, 118.1, 116.5, 114.1, 74.2, 62.8, 49.8, 45.1, 14.0.

Method B. Synthesis of 3-Cyanopyrazolo[1,5-*a*]quinoline (22) and 3-Cyano-4-hidroxypyridazo[1,6-*a*]quinolinium Inner Salt (23). To a solution of 1-amino-2-ethoxycarbonylquinolinium mesitylensulfonate **3c** (0.42 g, 1 mmol) and acrylonitrile (0.075 mL, 1.1 mmol) in dry CH_3CN (10 mL) was added *N*-ethyldiisopropylamine (0.35 mL, 2 mmol) dropwise. The reaction mixture was refluxed for 20 h, the solvent removed, and the residue chromatographed on silica gel (hexane/EtOAc 9:1 as eluent). **22** (0.116 g, 61%) was eluted first and isolated as a pale yellow solid: mp 143−144 °C (hexane/EtOAc) lit.[19] 145 °C (MeOH); IR (KBr) 3417, 2222, 1617, 1547, 1201, 1135 cm^{-1}; ^{1}H NMR ($CDCl_3$, 300 MHz) δ 8.62 (d, 1H, J = 8.1 Hz), 8.29 (s, 1H), 7.90 (d, 1H, J = 7.7 Hz), 7.84−7.76 (m, 1H), 7.77 (d, 1H, J = 9.3 Hz), 7.67 (d, 1H, J = 9.3 Hz); ^{13}C NMR ($CDCl_3$, 50 MHz) δ 143.9, 140.9, 134.3, 130.8, 129.0, 128.7, 126.3, 123.5, 116.1, 114.3, 113.8, 85.2; MS (*m*/*z*) 193 (M^+, 100).

23 (8 mg, 4%) was obtained as a yellow solid eluting with EtOAc: mp 273−275 °C; IR (KBr) 2931, 2212, 1733, 1643, 1542, 1312, 1261 cm^{-1}; ^{1}H NMR ($CDCl_3$, 300 MHz) δ 9.24 (d, 1H, J = 8.8 Hz), 8.77 (d, 1H, J = 9.2 Hz), 8.66 (s, 1H), 8.43 (d, 1H, J = 9.2 Hz), 8.16−8.03 (m, 2H), 7.98−7.91 (m, 1H); MS (*m*/*z*) 221 (M^+, 35), 195 (100).

Reaction of 1-Ethoxycarbonylisoquinolinium *N*-Aminide with Acrylonitrile. Synthesis of 1-Cyanopyrazolo[5,1-*a*]isoquinoline (26). To a solution of 2-amino-1-ethoxycarbonyl isoquinolinium mesitylensulfonate **3c** (0.42 g, 1 mmol) and acrylonitrile (0.075 mL, 1.1 mmol) in dry CH_3CN (10 mL) was added *N*-ethyldiisopropylamine (0.35 mL, 2 mmol) dropwise. The reaction mixture was refluxed for 48 h, the solvent removed, and the residue chromatographed on silica gel (hexane/EtOAc 1:1 as eluent); 0.045 g (23%) of **26** was obtained as a white solid: mp 144−145 °C (hexane/EtOAc). lit.[19] 147 °C (EtOH); ^{1}H NMR ($CDCl_3$, 200 MHz) δ 8.80−8.66 (m, 1H), 8.27 (d, 1H, J = 7.4 Hz), 8.21 (s, 1H), 7.85−7.75 (m, 1H), 7.75−7.60 (m, 2H), 7.21 (d, 1H, J = 7.4 Hz).

Acknowledgment. We are grateful to the Comisión Interministerial de Ciencia y Tecnologia (CICYT, projet PM97-0074) for financial support and to the Ministerio de Educación y Ciencia for a grant to one of us (J.V.M). We also thank to Profs. J.L. Abboud and J.L. Andres for careful reading of the manuscript and helpful discussions.

JO9909655

(19) Tominaga, Y.; Ichihara, Y.; Mori, T.; Kamio, C.; Hosomi, A. *J. Heterocycl. Chem.* **1990**, *27*, 263.